NeuroImage 279 (2023) 120326

Contents lists available at ScienceDirect

NeuroImage

journal homepage: www.elsevier.com/locate/ynimg

The dorsomedial prefrontal cortex represents subjective value across effort-based and risky decision-making

Yuan-Wei Yao [a,b,c,d,*], Kun-Ru Song [e], Nicolas W. Schuck [d,f,g], Xin Li [e], Xiao-Yi Fang [h], Jin-Tao Zhang [e,*], Hauke R. Heekeren [a,i], Rasmus Bruckner [a,d]

[a] Department of Education and Psychology, Freie Universität Berlin, Berlin, Germany
[b] Einstein Center for Neurosciences Berlin, Charité – Universitätsmedizin Berlin, Germany
[c] Department of Systems Neuroscience, University Medical Center Hamburg-Eppendorf, Hamburg, Germany
[d] Max Planck Research Group NeuroCode, Max Planck Institute for Human Development, Berlin, Germany
[e] State Key Laboratory of Cognitive Neuroscience and Learning and IDG/McGovern Institute for Brain Research, Beijing Normal University, Beijing, China
[f] Max Planck UCL Centre for Computational Psychiatry and Ageing Research, Berlin, Germany
[g] Institute of Psychology, Universität Hamburg, Hamburg, Germany
[h] Institute of Developmental Psychology, Beijing Normal University, Beijing, China
[i] Executive University Board, Universität Hamburg, Hamburg, Germany

ARTICLE INFO

Keywords:
Effort
Risk
Decision-making
Subjective value
Dorsomedial prefrontal cortex
fMRI

ABSTRACT

Decisions that require taking effort costs into account are ubiquitous in real life. The neural common currency theory hypothesizes that a particular neural network integrates different costs (e.g., risk) and rewards into a common scale to facilitate value comparison. Although there has been a surge of interest in the computational and neural basis of effort-related value integration, it is still under debate if effort-based decision-making relies on a domain-general valuation network as implicated in the neural common currency theory. Therefore, we comprehensively compared effort-based and risky decision-making using a combination of computational modeling, univariate and multivariate fMRI analyses, and data from two independent studies. We found that effort-based decision-making can be best described by a power discounting model that accounts for both the discounting rate and effort sensitivity. At the neural level, multivariate decoding analyses indicated that the neural patterns of the dorsomedial prefrontal cortex (dmPFC) represented subjective value across different decision-making tasks including either effort or risk costs, although univariate signals were more diverse. These findings suggest that multivariate dmPFC patterns play a critical role in computing subjective value in a task-independent manner and thus extend the scope of the neural common currency theory.

1. Introduction

The ability to weigh rewards and costs is critical for optimal decision-making (Frömer and Shenhav, 2021; Lopez-Gamundi et al., 2021; Westbrook et al., 2020). Physical effort is a common type of cost associated with our daily activities (Klein-Flügge et al., 2016; Sayalı and Badre, 2019), such as exercising (Harris and Bray, 2021) and helping others (Lockwood et al., 2017). Furthermore, imbalanced effort sensitivity appears to be a key feature of multiple disorders, including schizophrenia (Gold et al., 2015), binge eating (Brassard and Balodis, 2021), and depression (Treadway et al., 2012). Considering the ubiquitous presence of physical effort in our daily life and its clinical relevance, it is crucial to elucidate the cognitive and neural mechanisms underlying effort-based valuations.

The neural common currency theory suggests that a particular neural network is involved in subjective value calculation on a common scale across multiple decision situations (Levy and Glimcher, 2012; Sescousse et al., 2013), thus providing a powerful framework to explain how different options are compared in the brain. Indeed, several lines of research have shown a positive association between ventromedial prefrontal cortex (vmPFC) activity and subjective value in decisions that involve other types of costs, such as risk and delay (Bartra et al., 2013; Kable and Glimcher, 2007; Peters and Büchel, 2009). Hence, the vmPFC has been proposed as a central node of this domain-general valuation network (Levy and Glimcher, 2012; Sescousse et al., 2013; Smith et al., 2010).

* Corresponding authors.
E-mail addresses: yywyao@gmail.com (Y.-W. Yao), zhangjintao@bnu.edu.cn (J.-T. Zhang).

https://doi.org/10.1016/j.neuroimage.2023.120326
Received 16 March 2023; Received in revised form 9 August 2023; Accepted 11 August 2023
Available online 12 August 2023

While this view has also received some supportive evidence in effort-based decision-making (Hogan et al., 2019; Westbrook et al., 2019), a few other studies have identified effort-related value signals beyond the vmPFC (Chong et al., 2017; Klein-Flügge et al., 2016), particularly in a more dorsal portion of the medial prefrontal cortex (dmPFC) that mainly includes the dorsal anterior cingulate cortex (dACC) and some parts of the pre-supplementary motor area (Kolling et al., 2016; Piva et al., 2019). A meta-analysis showed that both vmPFC and dmPFC activity are associated with effort-reward integration, although in opposite directions (Lopez-Gamundi et al., 2021). These findings thus raise the possibility that, next to its ventral counterpart, the dmPFC also plays an important role in computing the subjective value of effortful options.

To date, only a few studies with divergent results have directly tested if the neural common currency theory could be applied to effort-based decision-making by comparing it with other decisions that require cost-reward integration (Aridan et al., 2019; Massar et al., 2015; Prévost et al., 2010; Seaman et al., 2018). For example, one study found neural correlates of value in the vmPFC during both effort-based and risky decision-making (Aridan et al., 2019), whereas some other studies showed that the dmPFC was uniquely involved in effort-reward integration (Massar et al., 2015; Prévost et al., 2010). One possible factor that may have caused this inconsistency is that some studies required participants to exert effort during decision-making, while others did not, possibly confounding neural correlates of subjective value with motor execution effects (Chong et al., 2017; Lopez-Gamundi et al., 2021). Moreover, different computational models were used to describe effort-reward integration, which may influence the estimation of trial-by-trial subjective value and its neural correlates (Prévost et al., 2010; Klein-Flügge et al., 2015; Chong et al., 2017; Arulpragasam et al., 2018). Finally, those studies mainly relied on a mass-univariate approach, which ignores the dependencies between brain voxels, as opposed to multivariate pattern analyses (Haynes and Rees, 2006). Therefore, studies solely based on univariate analyses might be less sensitive to detecting value signals in heterogeneous regions like the medial prefrontal cortex (Jimura and Poldrack, 2012; Kahnt, 2018; Nee et al., 2011).

The current study aimed to directly test the neural common currency theory by examining which brain regions represent subjective value across effort-based and risky decision-making. Unlike previous studies, we used a combination of computational modeling and both univariate and multivariate fMRI analyses. Accordingly, we first reanalyzed an existing dataset (Aridan et al., 2019) and then conducted an independent study to confirm our results. We found that multivariate dmPFC patterns consistently represented subjective value across effortful and risky tasks, and such effects may be neglected by univariate analyses. Our results might help reconcile current debates on the neural basis of effort-based valuation and extend the scope of the neural common currency theory to include the dmPFC as a critical region in the domain-general valuation network.

2. Materials and methods

2.1. Study 1

2.1.1. Participants

We used the behavioral and fMRI data of the effort-based and risky decision-making tasks from the study of Aridan et al. (2019), in which the details of the participant data were reported. Briefly, forty (twenty-one female) healthy, right-handed participants were enrolled in this study. One participant was excluded from the effortful task because they showed significant gain-aversive and loss-seeking behavior. Data from two participants were excluded because they showed extreme choice behaviors (i.e., accepted or rejected more than 90% of gambles) during the risky task. Therefore, the final dataset included 39 and 38 participants for effort-based and risky decision-making, respectively. The experiment was approved by the Institutional Review Board of the University of Texas at Austin, and all participants provided written informed consent prior to the experiment.

2.1.2. Experimental paradigm

Prior to scanning, participants were required to complete an effort-calibration task to measure their maximum voluntary contraction (MVC) and an association task to establish the relationship between cost levels and cues used in subsequent decision-making (Fig. 1a). Both decision-making tasks used during scanning were based on a one-option mixed-gamble paradigm.

For effort-based decision-making (Fig. 1b), each gamble included three components: a potential gain ($2-$12, in $2 increments), a potential loss ($1-$6, in $1 increments), and a physical effort requirement (30, 40, 50, 60, and 70% MVC). Participants were asked whether they would like to accept a gamble by indicating one of the four responses (strongly accept, weakly accept, weakly reject, and strongly reject), which were collapsed into accept and reject categories in subsequent analyses. Each task included 180 trials based on the unique combination of these three components. The task was split into five runs, with 36 trials each. Participants were instructed that they did not need to execute the required effort during the task. Instead, a trial would be randomly picked at the end of the task. If it was accepted, participants had to squeeze a dynamometer to reach the corresponding effort requirement. The outcome (gain or loss) was determined by their successful effort performance. If the gamble was rejected, participants would not receive any outcome from this task.

The risky decision-making task had a similar task structure (Fig. 1c), except that the effort requirement was replaced by the winning probability (90, 70, 50, 30, and 10%). Again, a trial was randomly picked at the end, and the outcome was based on the partcipants' choice (accept or reject) and winning probability.

2.1.3. MRI data acquisition

The neuroimaging data are openly available at https://openneuro.org/datasets/ds003782. They were collected on a 3T Siemens Skyra MRI scanner (Siemens, Erlangen, Germany). Scanning parameters were reported in Aridan et al. (2019). Functional images were collected with a T2*-weighted multiband echo-planar imaging (EPI) pulse sequence (TR = 1000 ms, multiband acceleration factor = 4, iPAT parallel acceleration factor = 2, TE = 30 ms, flip angle = 63°, FOV = 230, voxel size = 2.4 × 2.4 × 2.4 mm, 56 slices). These data were acquired at an angle of 30° off the anterior commissure-posterior commissure (AC-PC) line to reduce signal dropout in the orbitofrontal region (Deichmann et al., 2003). A high-resolution T1-weighted anatomical image was collected using a MPRAGE pulse sequence (TR = 1900 ms, TE = 2.43 ms, flip angle = 9°, FOV = 256, voxel size = 1.0 × 1.0 × 1.0 mm).

2.2. Study 2

2.2.1. Participants

Thirty-six (twenty female) healthy, right-handed participants were enrolled in this study. All participants had normal or corrected-to-normal vision, fulfilled all eligibility criteria for participating in an fMRI study, and reported no history of psychiatric or neurological disorders. Five participants were excluded from the subsequent experiment because of extreme choice behaviors (i.e., accepted or rejected more than 90% of effortful or risky options) during the pre-scanning tests. Another participant was excluded from the effortful task during scanning because they showed significant gain-aversive and loss-seeking behavior. Therefore, the final dataset included 30 and 31 participants for effort-based and risky decision-making, respectively. After the experiment, participants received financial compensation based on their participation time and randomly selected chosen options from the decision-making tasks. The experiment was approved by the Ethics Committee of the Department of Education and Psychology of Freie Universität Berlin, and all participants provided written informed

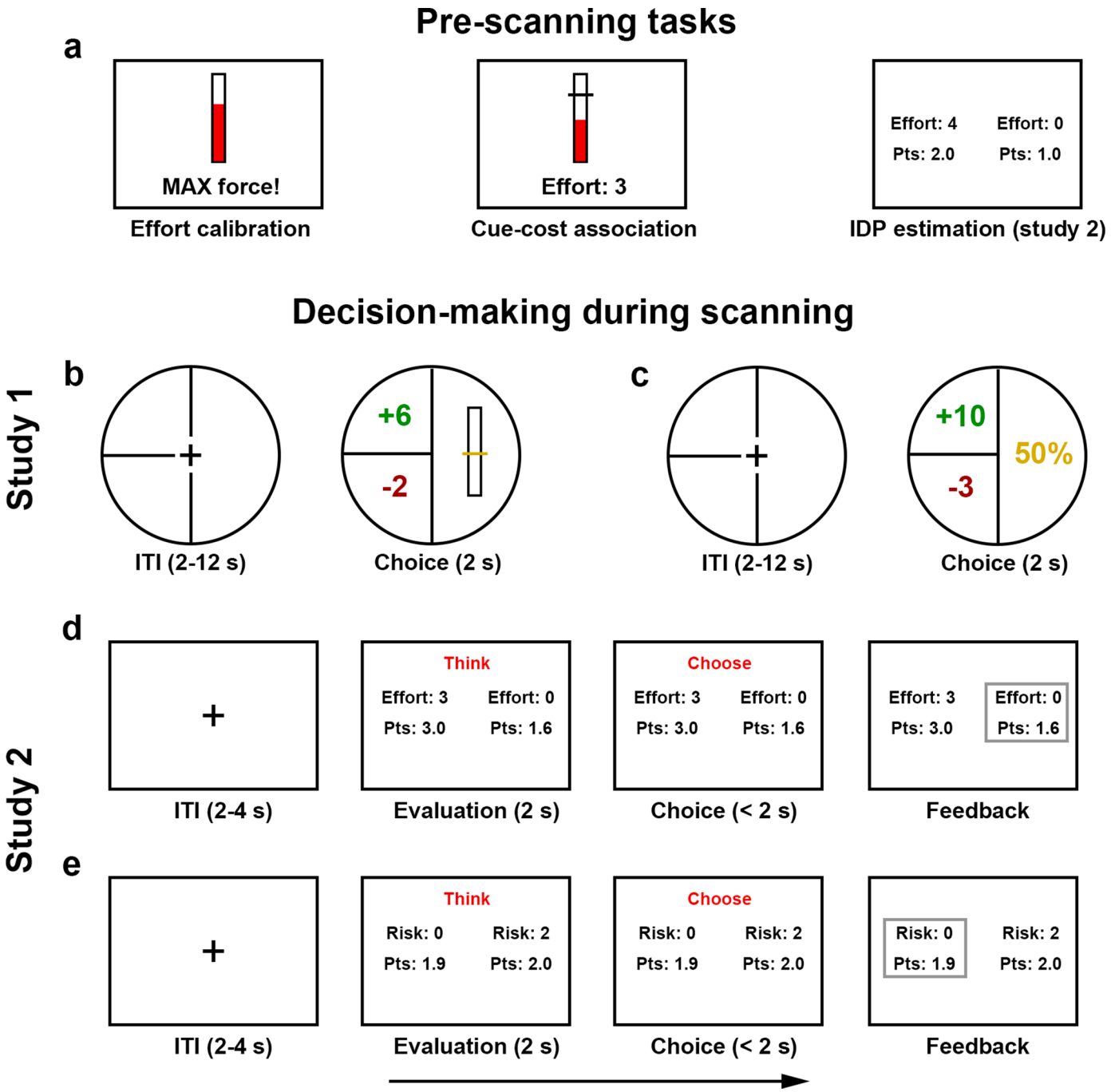

Fig. 1. Experimental design overview. (a) Prior to scanning, participants were asked to complete an effort-calibration task and a cue-effort association training. In study 2, participants need to do an additional task to estimate indifference points (IDP) for all combinations of rewards and cost levels (effort or winning probability). In study 1, (b) one-option effort-based and (c) risky decision-making tasks were conducted during scanning. Each trial included three components: a potential gain, a potential loss, and a cost. In study 2, (d) two-option effort-based and (e) risky decision-making were conducted in the scanner. The amount of the smaller reward was determined by the indifference point of the large-reward option (as determined in the IDP task) and a proximity value ($small\ reward = IDP \cdot (1 + \gamma)$).

consent prior to the experiment.

2.2.2. Experimental paradigm

The purpose of study 2 was to replicate the key findings of study 1 and to address some potential issues related to the experimental design. Specifically, we modified the experimental task in order to: (1) have a similar overall acceptance rate of high-cost options between effort-based and risky decision-making; (2) separate the evaluation and action selection phases during decision-making; (3) reduce the collinearity between subjective value and decision difficulty; and (4) reduce the involvement of the risk component in effort-based decision-making by removing the time limit of effort execution and potential losses during decision-making.

Specifically, for effort-based decision-making, participants were required to complete three tasks outside the scanner (Fig. 1a): First, a calibration task was conducted to measure participants' MVC. Participants were asked to squeeze the dynamometer (Vernier HD-BTA, Beaverton, USA) using their right hand as hard as possible for 6 s, followed by a rest period of 5 s. This procedure was repeated five times, and the MVC was defined as the averaged force above the median point over the

last half of the squeezing period across these five trials (Meyniel et al., 2016). Second, participants were trained to remember four associations between effort level cues (level 1–4) and physical effort requirements (50, 65, 80, 95% MVC), because the effort level cues would be used in the subsequent effort-based decision-making task. In each trial, participants were presented an effort level cue. Subsequently, they were shown a thermometer with a yellow line as the required force level and the height of the red filling as the real-time squeezing force. Unlike study 1, participants were required to keep the red filling above the yellow line for a total of 6 s. Although participants were asked to reach the effort requirement as quickly as possible, there was no time limit for effort execution. Therefore, participants could successfully complete all effort requirements in study 2. Each cue-effort association was repeated twice, yielding eight trials in total. Third, participants made a series of choices to estimate indifference points based on a previously validated procedure (Westbrook et al., 2013). In each trial, participants were asked to choose between an option associated with a larger reward (2, 3, or 4 points) and an effort requirement (level 1–4) and an alternative with a smaller reward but no effort requirement. The amount of the smaller reward was changed in a stepwise titration manner (6 iterations for each unique combination of effort and larger reward) until the two options were indifferent to participants (see Supplementary Methods and Figure S1 for details).

After the three pre-scanning tasks, another effort-based decision-making task was conducted in the scanner, which is the focus of this paper. Participants were asked to complete another two-option decision-making task (Fig. 1d). To control the overall acceptance rate of effortful options and to ensure sufficient variability in choice behavior, we varied the amount of the smaller reward (SR) around the indifference point (IDP) of the corresponding larger-reward option using a proximity parameter γ (Westbrook et al., 2019):

$$SR = IDP \cdot (1 + \gamma) \tag{1}$$

Therefore, the absolute value of γ specified the subjective value difference between the two options. A positive value indicated that the effortless option was favored and vice versa. Each run of the task included 48 slightly biased trials (unique combination of proximity parameter value from {−0.4, −0.1, 0.2, 0.5}, effort requirement, and large reward) and eight strongly biased trials (unique combination of proximity parameter value from {−0.8, 0.8} and effort requirement, randomly paired with a large reward). The amount of the smaller reward would not exceed that of the larger reward.

This task included three runs and a total of 168 trials. In each trial, to isolate the motor component from the valuation process, participants were presented with two options for 2 s (evaluation period) first before getting the notice to make a choice within 2 s (action period). A 2–4 s interval was used between trials (ITI). At the end of the task (outside of the scanner), ten trials were randomly selected. If participants chose the effortful option, they could only get the rewards after exerting the required effort by squeezing the dynamometer.

The risky decision-making part was implemented in a similar procedure, except that the calibration task was not required and that four risk levels were associated with four winning probabilities (90, 70, 50, 30%). A two-option risky decision-making task (168 trials; Fig. 1e) was conducted in the scanner. Again, ten trials were randomly selected at the end of the task outside the scanner. Participants were shown the outcome of each trial generated by the computer based on the winning probability. The order of the effort-based and risky decision-making tasks was counterbalanced across participants.

2.2.3. MRI data acquisition

MRI data were acquired using a 3T Siemens Trio scanner (Siemens, Erlangen, Germany). Functional images were collected with a T2*-weighted EPI pulse sequence (TR = 2000 ms, TE = 25 ms, flip angle = 85°, FOV = 220, voxel size = 3.4 × 3.4 × 4.0 mm, 34 slices). A high-resolution T1-weighted anatomical image was collected using a MPRAGE pulse sequence (TR = 2530 ms, TE = 3.39 ms, flip angle = 7°, FOV = 256, voxel size = 1.3 × 1.0 × 1.3 mm, 144 slices).

2.3. MRI data preprocessing

MRI data of both datasets were preprocessed using SPM12 (version 7177; https://www.fil.ion.ucl.ac.uk/spm/software/spm12/) and DPABI (Yan et al., 2016) in MATLAB (version 2019b; http://www.mathworks.com/). Functional images were corrected for motion through realignment with respect to the first volume. Both functional and anatomical images were manually checked and reoriented based on the AC-PC line before they were co-registered. The anatomical images were then segmented into gray matter, white matter, and cerebrospinal fluid. Finally, functional images were normalized to Montreal Neurological Institute (MNI) space and smoothed using a Gaussian kernel with 6-mm full-width-half-maximum (FWHM). Participants who showed excessive head motion (i.e., > 3 mm of displacement or 3° of rotation in any of the six head motion parameters from realignment) in more than two runs of a task were excluded from subsequent analyses.

2.4. Computational modeling of choice behaviors

Behavioral data were analyzed using R (version 4.1.2; https://cran.r-project.org/). For effort-based decision-making, we used five different discounting functions used in previous studies (Arulpragasam et al., 2018; Chong et al., 2017; Klein-Flügge et al., 2015; Prévost et al., 2010) to characterize the way that a prospective outcome is devalued by effort (Figure S2), which were defined as follows:

$$Linear: \ SV = OC - k \cdot E \tag{2}$$

$$Hyperbolic: \ SV = OC \cdot \frac{1}{1 + k \cdot E} \tag{3}$$

$$Parabolic: \ SV = OC - k \cdot E^2 \tag{4}$$

$$Two-parameter\ power: \ SV = OC - k \cdot E^p \tag{5}$$

$$Sigmoidal: \ SV = OC \cdot \left(1 - \left(\frac{1}{1 + e^{-k \cdot (E - tp)}} - \frac{1}{1 + e^{k \cdot tp}}\right) \cdot \left(1 + \frac{1}{e^{k \cdot tp}}\right)\right) \tag{6}$$

where k is a free parameter, which reflects the discounting rate. The two-parameter power function has another free parameter p that reflects effort sensitivity. The sigmoidal function has another free parameter tp that determines the turning point of the curve (Klein-Flügge et al., 2015). E denotes the objective effort requirement (e.g., 0.3, 0.4, 0.5, 0.6, 0.7 for dataset 1). OC denotes the outcome. For study 1, it is defined as eq. (7), where λ reflects the relative weighting of losses and gains, and α reflects outcome sensitivity.

$$OC = Gain^{\alpha} - \lambda \cdot Loss^{\alpha} \tag{7}$$

For study 2, since options are not associated with potential losses, OC equals the potential gain value.

$$OC = Gain^{\alpha} \tag{8}$$

Models for risky decision-making have already been extensively studied in previous work (Kahneman and Tversky, 1979; Nilsson et al., 2011; Pachur et al., 2017; Tversky and Kahneman, 1992; Von Neumann and Morgenstern, 1944). Therefore, we examined two models based on the original and cumulative prospect theory to calculate trial-wise subjective value during risky decision-making.

The original perspective theory (PT, Kahneman and Tversky, 1979) proposes that the subjective value of a risky option is defined as:

$$SV = Gain^{\alpha} \cdot p - \lambda \cdot Loss^{\alpha} \cdot q \tag{9}$$

where p and q are the winning and losing probability, respectively. For

study 2, only the part related to gains was used:

$$SV = Gain^{\alpha} \cdot p \tag{10}$$

The cumulative prospect theory (CPT; Tversky and Kahneman, 1992) further transforms objective probabilities into subjective probabilities:

$$SV = Gain^{\alpha} \cdot w^{+}(p) - \lambda \cdot Loss^{\alpha} \cdot w^{-}(q) \tag{11}$$

The weighting functions for gains and losses (w^{+} and w^{-}) are defined as:

$$w^{+}(p) = \frac{\delta^{+} \cdot p^{\gamma}}{\delta^{+} \cdot p^{\gamma} + (1-p)^{\gamma}}$$

$$w^{-}(q) = \frac{\delta^{-} \cdot q^{\gamma}}{\delta^{-} \cdot q^{\gamma} + (1-q)^{\gamma}} \tag{12}$$

The parameter γ controls the curvature of the weighting function. The parameters $\delta^{+}$and δ^{-}control the elevation of the weighting function for gains and losses, respectively (Pachur et al., 2017).

For both tasks, the softmax function was used to calculate the probability of choosing the effortful or risky option:

$$P(A,B) = \frac{e^{\beta \cdot SV(A)}}{e^{\beta \cdot SV(A)} + e^{\beta \cdot SV(B)}} \tag{13}$$

where $P(A,B)$ is the choice probability of choosing (costly) option A over (no-cost) option B. β denotes the stochasticity of a participant's choice. $SV(A)$ and $SV(B)$ represent the subjective value of option A and B, respectively. Please note that $SV(B)$ is always 0 in study 1 and the amount of the smaller reward in study 2.

All models were fitted and evaluated using a hierarchical Bayesian approach by following the template used in the hBayesDM package (Ahn et al., 2017). Because this method not only estimates parameters for each participant but also includes a group-level hyperparameter distribution that governs the individual-level parameters, it is less sensitive to outliers and can generate more robust estimates (Huys et al., 2011; Lockwood and Klein-Flügge, 2021). The parameter estimation was conducted using Monte-Carlo Markov Chain (MCMC) sampling implemented in Stan (version 2.21; https://mc-stan.org/). We used four chains, each with 2000 MCMC samples, including a burn-in period of 1000 samples. To determine which model fit the data best, we used the loo package (version 2.4.1; https://cran.r-project.org/web/packages/loo/) to perform a model comparison based on the leave-one-out information criterion (LOOIC; Vehtari et al., 2017), which is a Bayesian criterion to evaluate the out-of-sample predictive performance of a model. A lower LOOIC indicates a better fit between the model and data. Model weight was also calculated using Bayesian model averaging based on Bayesian bootstrapping, with a higher weight indicating a higher probability of a model having generated the data (Yao et al., 2018).

Finally, to assess the validity of the winning model, we further conducted posterior predictive checks and checked if the posterior prediction from the model could capture key features of the behavioral data (Zhang et al., 2020). Moreover, we performed parameter recovery analyses to examine if the parameters of the winning model could be accurately identified (Wilson and Collins, 2019).

2.5. fMRI data analysis

2.5.1. Univariate analysis

To replicate the main findings reported in Aridan et al. (2019), we first conducted the model-based univariate fMRI analysis, in which the subjective value of each option was derived based on the winning model. For study 1, we focused on the choice period. Two general linear models (GLM1.1 and GLM1.2) were used to examine the neural activity related to the subjective value of each option during effort-based and risky decision-making, respectively. These models included two regressors using a stick function: high- and low-value trials, which were split based on the median subjective value. We used the contrast of high- vs. low-value at the first level. Moreover, another two GLMs (GLM1.3 and GLM1.4 for the effort-based and risky decision-making task, respectively) similar to the ones used in the original study were also conducted for confirmatory purposes (Aridan et al., 2019). These models included a regressor of the choice period of all trials and trial-by-trial subjective values as a parametric modulator. We focused on the effect of this parametric modulator at the first level.

In study 2, to isolate the effects of motor action on valuation, we divided each choice into evaluation and action periods. In subsequent analyses, we focused on the evaluation period and included the action period as a separate regressor of no interest. Because there are two options in each trial, we derived the subjective value of the chosen option from the winning model, consistent with other two-option decision-making studies (Arulpragasam et al., 2018; Hogan et al., 2019). We repeated the analyses used for study 1 but split trials based on the median chosen subjective value for GLM2.1 and GLM2.2. To facilitate the comparison across studies, we also conducted another two supplementary GLMs (GLM2.3 and GLM2.4) by including trial-wise chosen subjective value as a parametric modulator.

In all GLMs, trials without any responses were modeled as a separate nuisance regressor. Moreover, six motion parameters from the realignment were included as regressors of no interest. Contrasts from the first-level analyses were taken to group-level random-effects analyses. Voxelwise analyses were conducted within a frontostriatal mask, including Brodmann area (BA) 9, 10, 11, 23, 32 and bilateral nucleus accumbens, caudate, and putamen from the Harvard-Oxford structural atlas, which covered most potential regions within the valuation network (Bartra et al., 2013; Clithero and Rangel, 2014; Lopez-Gamundi et al., 2021) and excluded most sensory and motor areas. Statistical maps were corrected for multiple comparisons using a voxel-level uncorrected threshold of $p < 0.001$ and a FWE cluster-level corrected at $p < 0.05$ by means of Gaussian Random Field Theory (GRFT). Since we were particularly interested in the roles of the vmPFC and dmPFC in cost-reward integration, we extracted the mean effects from 6-mm-radius spherical masks of the vmPFC (coordinate: 0, 40, −4; Clithero and Rangel, 2014) and dmPFC (coordinate: 0, 22, 38; Piva et al., 2019; Venkatraman et al., 2009) for illustration.

2.5.2. Multivariate decoding analysis

Multivariate decoding analysis, which is the focus of this manuscript, was performed using a linear support vector machine (SVM) algorithm for binary classification implemented in The Decoding Toolbox (TDT, v 3.999E; Hebart et al., 2015). In study 1, we repeated the above mentioned first-level analyses on unsmoothed data and used the beta images from the choice period of GLM1.1 and GLM1.2 to examine neural representations of subjective value during effort-based and risky decision-making, respectively. For each task, a five-fold cross-run validation was used, in which the SVM was trained on all but one run and tested on the left-out run. We utilized the searchlight analysis (radius = 3 voxels) within the frontostriatal mask used in the univariate analyses above. Voxelwise cross-validated decoding accuracy (minus chance-level accuracy) was calculated.

To examine subjective value representations independent of cost types, we further conducted a cross-task decoding analysis, which included the beta images from both GLM1.1 and GLM1.2. The SVM was trained on four runs of one task (e.g., run 1–4 of the effort-based decision-making task) and tested on one run of the other task (e.g., run 5 of the risky decision-making task), and the procedure was repeated ten times.

For study 2, because both decision-making tasks only included three runs, each run was divided into two halves (i.e., six datasets for each task) to increase the number of datasets used for the decoding analyses (Jimura and Poldrack, 2012). GLM2.1 and GLM2.2 were performed on unsmoothed data, and beta images from the evaluation period were used for searchlight decoding analyses for each task. The cross-task decoding

analysis was also conducted as described above in study 1.

Since subjective value is calculated based on the integration of related benefit and cost components, we further conducted separate multivariate decoding analyses to examine neural representations of these basic components. For effort-based decision-making, we used effort levels and outcomes as the dependent variables. For risky decision-making, because risk is an outcome-related cost that modulates its value (Klein-Flügge et al., 2015), we instead focused on risk and reward levels.

Finally, we have conducted some control analyses to ensure our multivariate findings are valid and robust: (1) In study 1, since participants were asked to reach the required effort level within a 2 s time window, they showed a lower success rate for high effort requirement (Aridan et al., 2019). To reduce the potential effects of risk on effort-based value integration, we repeated the multivariate decoding analyses on trials with only low or medium effort requirements (level < 4) and included the high-effort trials as a separate regressor of no interest; (2) Since we used a two-option decision paradigm in study 2, to examine if the results were influenced by the definition of the subjective value variable, we conducted another two supplementary multivariate decoding analyses based on subjective value difference (i.e., chosen – unchosen subjective value); (3) To ensure that the results were mainly driven by subjective value but not decision difficulty, we included an index of trial-wise decision difficulty (i.e., 1-$|\gamma|$) as a modulated regressor in the multivariate decoding analyses (Todd et al., 2013) for study 2. (5) We also conducted control analyses by including choice as a modulated regressor for study 2 and response time (RT) for both studies to control for potential confounding effects of these factors on value integration.

Within-task decoding results were corrected for multiple comparisons using a voxel-level uncorrected threshold of $p < 0.001$ and a FWE cluster-level corrected $p < 0.05$. For exploratory purposes, cross-task decoding analyses and other control analyses were corrected using a lenient threshold of voxel-level $p < 0.005$ and a FWE cluster-level corrected $p < 0.05$. Similar to the univariate analyses, we extracted the mean decoding accuracy from the vmPFC and dmPFC spherical masks, respectively. It should be noted that these ROI results reflect post-hoc signal extractions from the searchlight analyses but not *a priori* ROI-wise MVPA.

3. Results

3.1. Effects of effort and risk on choices

We first conducted two one-way analyses of variance (ANOVAs) to examine general effects of effort and risk on choices, respectively. In study 1, results (Fig. 2a) showed that participants' probability of accepting an option decreased with effort ($F_{(1.5, 58.1)} = 42.00$, $p < 0.001$, partial $\eta^2 = 0.53$) and risk levels ($F_{(2.0, 75.3)} = 140.21$, $p < 0.001$, partial $\eta^2 = 0.79$). Moreover, participants showed a higher overall acceptance rate in the effortful compared with the risky task ($F_{(1, 36)} = 36.38$, $p < 0.001$, partial $\eta^2 = 0.50$).

In study 2, where we used two pre-scanning tasks to estimate indifference points for all combinations of reward and effort/risk, we took these indifference points normalized based on the larger reward amounts (i.e., indifference point/larger reward) as the dependent variable for one-way ANOVAs. This normalization step allowed us to compare the results across participants on a common scale. Both effort ($F_{(2.3, 68.2)} = 101.10$, $p < 0.001$, partial $\eta^2 = 0.77$) and risk levels ($F_{(2.5, 74.5)} = 95.63$, $p < 0.001$, partial $\eta^2 = 0.76$) decreased participants' normalized indifference points (Figure S3). For tasks conducted in the scanner, since we manipulated the small reward amount around the indifference point of the high-cost option using a proximity parameter, participants showed comparable acceptance rates of around 50% for high-cost options between tasks ($F_{(1, 29)} = 0.98$, $p = 0.77$, partial $\eta^2 = 0.03$; Fig. 2b). Moreover, as shown in Fig. 2c, participants selected more high-cost options when they were favorable (i.e., positive proximity values) and chose them less frequently when no-cost options were more favorable (Effort: $F_{(2.8, 80.3)} = 166.71$, $p < 0.001$, partial $\eta^2 = 0.85$; Risk: $F_{(2.2, 66.1)} = 114.62$, $p < 0.001$, partial $\eta^2 = 0.79$). These experimental manipulations also decreased the high collinearity at the subject level in study 1 (Figure S4 and Table S1).

3.2. Behavioral modeling of effort- and risk-related value integration

For effort-based decision-making in study 1, model comparison results showed that choice behavior was best described by a model based on the two-parameter power function (Fig. 3). Importantly, although the effortful task used in study 2 had a different structure (e.g., two options and no losses involved), model comparisons showed that the two-parameter power discounting model also fit the data best.

Regarding risky decision-making, we examined two models based on the original and cumulative prospect theory, respectively (Kahneman and Tversky, 1979; Tversky and Kahneman, 1992). Model comparisons suggest that the CPT model performed better than the original PT model in both studies (ΔLOOIC = 33 and 135). Group-level means and 95% highest density intervals for each parameter were included in Tables S2.

Since the model comparison only provides insights into the relative performance of the models in the model space, we further examined the

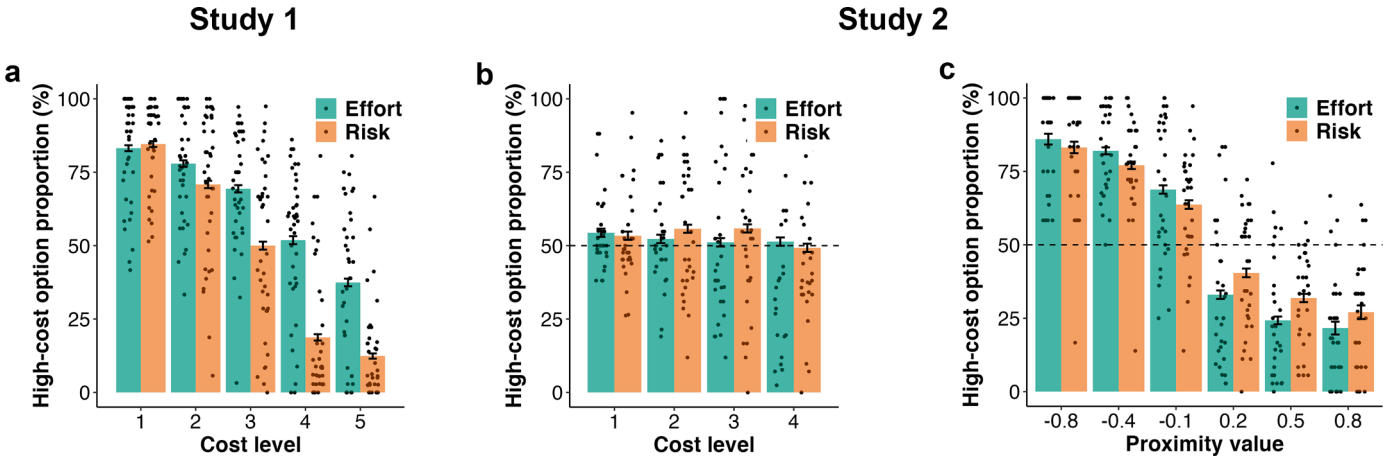

Fig. 2. Behavioral results. (a) In study 1, participants accepted less effortful and risky options when cost levels increased. (b) In study 2, since we manipulated the reward amount of the no-cost option around the indifference point for each high-cost option, the overall acceptance rate was around 50% for both tasks, and the acceptance rate did not change with cost levels. (c) The probability of choosing a high-cost option was influenced by the proximity value.

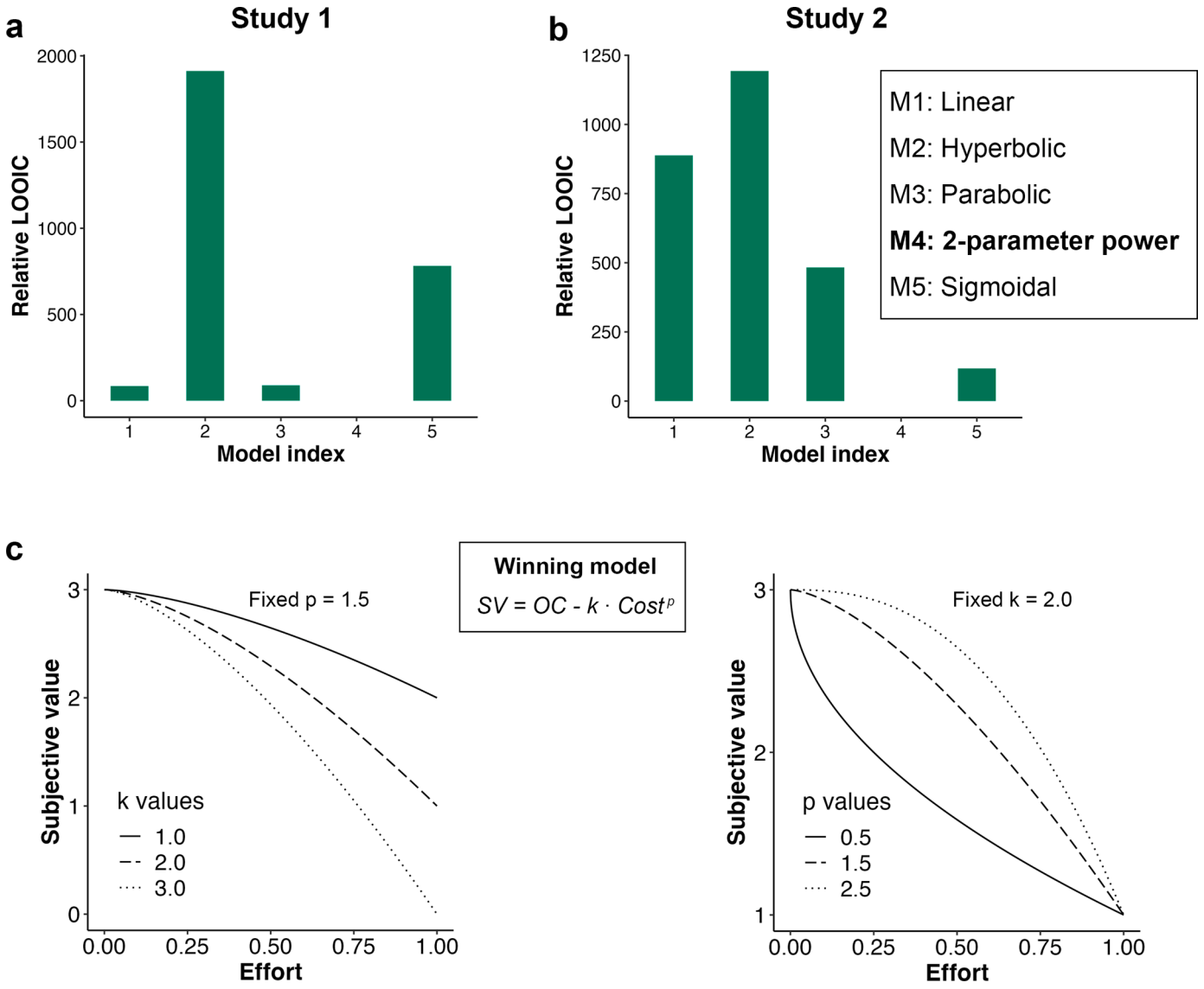

Fig. 3. Computational modeling of effort-based decision-making. (a) We compared the five discounting models (linear, hyperbolic, parabolic, two-parameter power, and sigmoidal) used in previous studies to describe how outcomes are devalued by effort costs. We found that the two-parameter power model showed the best fit in both studies. (b) Mathematical formula and graphical illustrations of the two-parameter power function. The graphs show that the combination of the two free parameters (discounting rate k and cost sensitivity p) can generate a wide range of discounting curves. *SV* and *OC* denote subjective value and outcome, respectively.

validity of the winning model based on separate posterior predictive checks for each task. We found that all winning models could generate posterior predictions that captured key features of the data (Figure S5). Additionally, we conducted parameter recovery analyses for the winning model for each task. The results showed that all group- and individual-level parameters could be accurately recaptured (Figure S6-S7).

3.3. Univariate neural correlates of subjective value

For effort-based decision-making (Fig. 4 and Table S3), we found that dmPFC activity was negatively associated with subjective value magnitude in both studies (study 1: $t(38) = -4.02$, $p < 0.001$, Cohen's $d = -0.64$; study 2: $t(29) = -5.07$, $p < 0.001$, Cohen's $d = -0.92$). Conversely, vmPFC activity was positively associated with subjective value in study 1 ($t(38) = 4.60$, $p < 0.001$, Cohen's $d = 0.74$), but this effect was not significant in study 2 ($t(29) = 0.02$, $p = 0.98$, Cohen's $d = 0$).

For risky decision-making (Fig. 4 and Table S3), in study 1, we found positive neural correlates of subjective value in the vmPFC ($t(37) = 2.25$, $p = 0.03$, Cohen's $d = 0.36$) but not dmPFC ($t(37) = 1.09$, $p = 0.29$, Cohen's $d = 0.18$). In study 2, we observed significant positive correlates of subjective value in a cluster in the dmPFC ($t(30) = 2.22$, $p = 0.03$, Cohen's $d = 0.40$) but not vmPFC ($t(30) = -1.87$, $p = 0.07$, Cohen's $d = -0.34$).

The above results are based on the categorical contrast of high vs. low subjective value, as the same GLMs were used in the subsequent multivariate decoding analyses. The main results could be qualitatively replicated by univariate analyses that included trial-wise subjective value as a parametric modulator (Figure S8).

3.4. Multivariate neural representations of subjective value

Since the univariate approach does not take dependencies between voxels into account, it may be less sensitive to detecting value-related signal in heterogeneous brain regions (Kahnt, 2018). To deal with this issue, we conducted searchlight multivariate decoding analyses within the same frontostriatal mask used in the univariate analyses. For

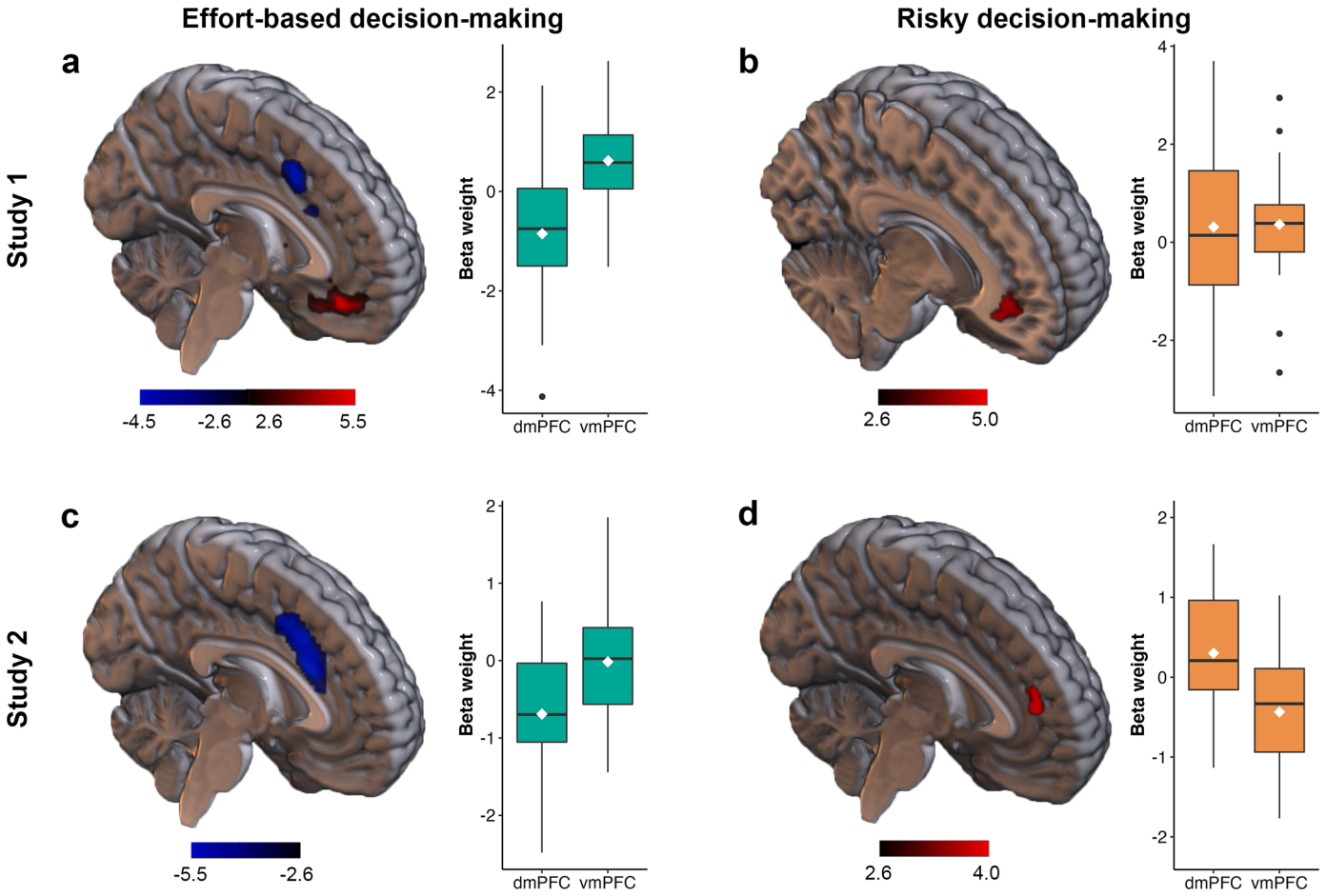

Fig. 4. Univariate neural correlates of subjective value. (a, b) In study 1, neural activity of the vmPFC was positively associated with subjective value in both tasks. In addition, dmPFC activity showed a negative association with subjective value. In study 2, (c) we observed some negative correlates of subjective value in the dmPFC during effort-based decision-making, (d) whereas the effect was opposite for risky decision-making.

effort-based decision-making, we found that subjective value information could be accurately decoded from a large cluster including both the vmPFC ($t(38) = 5.78$, $p < 0.001$, Cohen's $d = 0.93$) and dmPFC ($t(38) = 9.38$, $p < 0.001$, Cohen's $d = 1.50$) in study 1 (Table 1 and Fig. 5a). Additionally, we found that activity of the dmPFC also represented subjective value in study 2 (Figure 5c; $t(29) = 6.60$, $p < 0.001$, Cohen's $d = 1.20$), but the effect was not significant in the vmPFC ($t(29) = 1.43$, $p = 0.16$, Cohen's $d = 0.26$).

Similarly, for risky decision-making, subjective value information could be decoded in the vmPFC ($t(37) = 2.23$, $p = 0.03$, Cohen's $d = 0.36$) and dmPFC ($t(37) = 4.32$, $p < 0.001$, Cohen's $d = 0.70$) in study 1 (Table 1 and Fig. 5b). In study 2, we found that activity patterns of the vmPFC ($t(30) = 3.15$, $p = 0.004$, Cohen's $d = 0.57$) and dmPFC ($t(30) = 5.29$, $p < 0.001$, Cohen's $d = 0.95$) also represented subjective value information (Fig. 5d).

3.5. Cross-task subjective value encoding in the dmPFC

To directly test whether the dmPFC encodes value information in a task-independent manner, as suggested by the neural common currency theory (Kahnt, 2018), we utilized a cross-task multivariate decoding analysis (Table 1 and Fig. 6). Strikingly, we found that a cluster including the dmPFC ($t(36) = 4.26$, $p < 0.001$, Cohen's $d = 0.70$) and a small part of the vmPFC ($t(36) = 4.42$, $p < 0.001$, Cohen's $d = 0.73$) contained subjective value information independent of task type in study 1. In study 2, task-independent value information was mainly represented in the posterior dmPFC ($t(29) = 3.63$, $p < 0.001$, Cohen's $d = 0.66$), but not the vmPFC ($t(29) = -0.91$, $p = 0.37$, Cohen's $d = -0.17$).

Importantly, although the significant clusters from the two studies did not perfectly overlap, the above-chance decoding maps converged in a cluster in the dmPFC (Fig. 6c) at an uncorrected voxel-level threshold of $p < 0.005$. These findings thus provide support to the neural common currency theory and highlight the critical role of the dmPFC in subjective value representation across tasks and datasets.

3.6. Multivariate decoding analyses on benefit and cost terms

To examine whether the brain regions identified above can represent both benefit and cost terms related to subjective value, we conducted separate multivariate decoding analyses for these basic components for each task. For effort-based decision-making, we found that the dmPFC was involved in effort and outcome encoding in both studies (Figure S9). For risky decision-making, both studies showed that the risk information could be decoded from dmPFC neural patterns. In addition, we observed reward-related neural codes in the dmPFC in study 2, although this effect was not significant in study 1 (Figure S10).

3.7. Multivariate decoding control analyses

In study 1, we repeated the multivariate decoding analyses only on trials with low or medium effort requirements (level < 4) to reduce the involvement of risk associated with high-effort trials. Because we were still able to identify neural representations of subjective value in the dmPFC after excluding high-effort trials (Figure S11), this finding should not be attributed to risk processing.

Table 1
Within- and cross-task multivariate decoding results.

Analysis	Voxels	Region	BA	*t* value	MNI coordinates x	y	z
Study 1, effort task	3586	dmPFC/dlPFC	32	9.30	0	21	45
		Left precentral gyrus	9	6.21	−45	9	45
		Left frontal pole	10	5.81	−30	51	6
		vmPFC	10	5.63	3	51	0
	40	Right OFC	11	5.49	27	24	−21
Study 1, risk task	837	Right dlPFC/ dmPFC	32/ 9/24	6.52	27	33	42
	73	Right OFC	11	4.30	21	63	−12
Study 2, effort task	424	dmPFC	32	7.09	−9	24	48
Study 2, risk task	2205	dlPFC	9	7.10	−21	30	39
		dmPFC	32	6.70	−6	18	45
		Frontal pole	10/ 11	7.08	−24	54	0
		vmPFC	11/ 10	5.93	−9	42	−9
Study 1, cross tasks	699	dmPFC/dlPFC	10/ 32	4.50	−12	57	15
Study 2, cross tasks	144	dmPFC	32/ 24	3.80	−3	15	27

Within-task multivariate decoding results are corrected for multiple comparison using a voxel-wise uncorrected threshold of $p < 0.001$ and a FWE cluster-level corrected threshold of $p < 0.05$. For large clusters (i.e., voxel size > 2000), another three peak coordinates inside the cluster were reported. For exploratory purposes, cross-task multivariate decoding results are corrected using a voxel-wise threshold of $p < 0.005$ and a FWE cluster-level corrected threshold of $p < 0.05$.
dmPFC: dorsomedial prefrontal cortex; dlPFC: dorsolateral prefrontal cortex; vmPFC: ventromedial prefrontal cortex; OFC: orbitofrontal cortex.

In study 2, multivariate decoding results were based on chosen subjective value, to ensure that our findings were not influenced by the exact definition of the subjective value variable, we repeated all analyses using the subjective value difference of each trial as the dependent variable. These analyses yielded similar results as reported in the main analyses and showed that subjective value difference information could also be decoded from the neural patterns of the dmPFC (Figure S12).

Furthermore, previous work suggests that the dmPFC encodes choice difficulty beyond subjective value (Hogan et al., 2019; Shenhav et al., 2016; Westbrook et al., 2019). In study 2, we independently manipulated decision difficulty and chosen subjective value across trials, which thus allowed us to conduct multivariate decoding control analyses by including trial-wise decision difficulty (i.e., 1-$|\gamma|$) as a potential confounding variable (Todd et al., 2013). The decoding results remained qualitatively the same after controlling for the effects of decision difficulty (Figure S13). Moreover, to explore whether multivariate pattern activity in the dmPFC reflects choice difficulty, we performed decoding analyses on decision difficulty with subjective value as a modulated regressor. However, we did not observe any significant results in the dmPFC after controlling for the effects of chosen subjective value, suggesting that dmPFC neural patterns identified in this study were mainly driven by subjective value rather than decision difficulty.

Finally, we also conducted multivariate decoding analyses by including choice for study 2 and RT for both studies as a modulated regressor. Notably, neural codes of subjective value could be reliably decoded in all these control analyses (Figure S14-S15).

4. Discussion

We used behavioral modeling combined with univariate and multivariate fMRI analyses to examine the neural and computational mechanisms underlying effort-based and risky decision-making. We found that the two-parameter power discounting model showed the best fit for modeling effort-based decision-making. At the neural level, the multivariate decoding analyses consistently showed that the dmPFC represented subjective value information in a task-independent manner, although the effects may be undetectable in some univariate analyses. These findings further elucidate the neural response patterns within the medial prefrontal cortex during value integration and suggest that the dmPFC may serve as a potential hub in subjective value computations independent of the cost types.

Previous behavioral modeling studies have used different discounting functions to describe the way that effort devalues prospective outcomes, yet yielded mixed results (Arulpragasam et al., 2018; Chong et al., 2017; Klein-Flügge et al., 2015; Prévost et al., 2010). In the current study, we compared different discounting models used in previous research and found that the two-parameter power discounting model showed the best fit for effort discounting. A key feature of this model is that, next to the discounting-rate parameter k, it includes another free parameter p modeling effort sensitivity (Arulpragasam et al., 2018). Although a preliminary consensus is that effort discounting follows a concave shape at the group level, which can also be achieved by the parabolic or sigmoidal model (Chong et al., 2017; Klein-Flügge et al., 2015), a large amount of between-subject variability was often reported (Escobar et al., 2023). The effort sensitivity parameter p allows the power discounting function to flexibly generate a wide range of discounting shapes to account for individual differences in effort discounting.

At the neural level, there has been considerable debate over the exact role of the dmPFC, particularly the dACC area, in effort-reward integration (Arulpragasam et al., 2018; Chong et al., 2017; Hogan et al., 2019; Klein-Flügge et al., 2016; Westbrook et al., 2019). Although lesion studies in animals and non-invasive brain stimulation studies in humans suggest that the dmPFC is critically involved in effort-based decision-making (Rudebeck et al., 2008; Soutschek et al., 2022; Walton et al., 2009), fMRI studies in humans yielded rather divergent results (Arulpragasam et al., 2018; Chong et al., 2017; Hogan et al., 2019; Klein-Flügge et al., 2016). One potential explanation is that the association between dmPFC activity and subjective value is often negative when using univariate analyses (Lopez-Gamundi et al., 2021), which might have been overlooked by studies focusing on positive neural correlates. Moreover, neural activity within the dmPFC is highly heterogeneous (Neubert et al., 2015), which may cause the results to be undetectable when voxels within this region are treated as homogenous.

Therefore, one important advantage of the current study is that we utilized both univariate and multivariate analysis approaches. Indeed, for effort-based decision-making, we observed negative correlations with subjective value in the dmPFC using univariate analyses and significant neural coding of subjective value in this region using multivariate decoding analyses. Notable, within-task multivariate decoding consistently showed a larger effect size compared to the corresponding univariate analysis (Table S4). These findings are in line with a recent study that used representational similarity analysis, another multivariate method, to examine subjective value representations during effort-based decision-making (Lockwood et al., 2022). For risky decision-making, despite diverse univariate results in the dmPFC, multivariate patterns of this region consistently represented subjective value. These results are in keeping with a previous study based on intertemporal decision-making (Wang et al., 2014), in which MVPA yielded value codes in the dmPFC even in the absence of univariate effects. Taken together, these findings suggest that the dmPFC can represent subjective value based on distributed neural coding that may be beyond the detectability of univariate analyses.

Cross-task multivariate decoding is especially suited to test whether a brain region represents subjective value using similar neural patterns in different tasks at the subject level (Kahnt, 2018). This analysis yielded a significant dmPFC cluster in both studies, suggesting that subjective

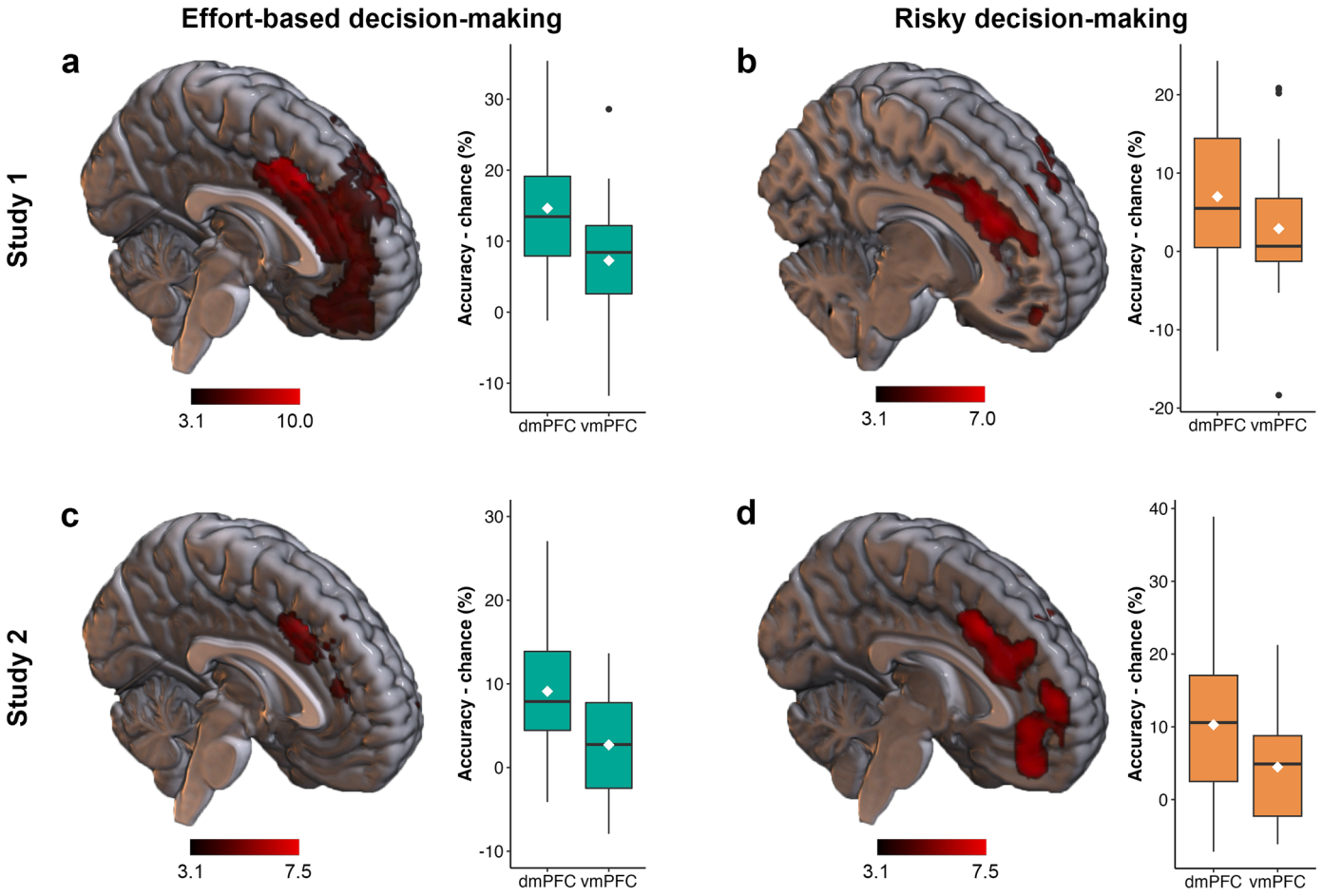

Fig. 5. Within-task multivariate decoding results. (a, b) In study 1, the dmPFC and vmPFC represented subjective value in both tasks, although the vmPFC cluster was only detectable before multiple comparison correction. (c, d) In study 2, subjective value could also be decoded from the dmPFC in both tasks, and the cluster identified in the risky decision-making task extended to the vmPFC.

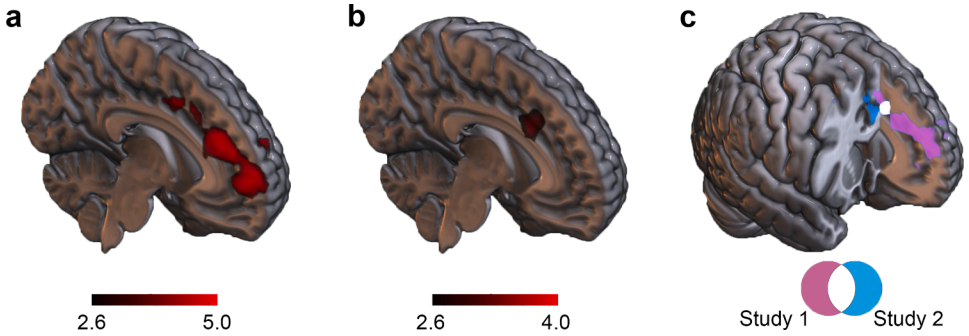

Fig. 6. Cross-task multivariate neural representations of subjective value. (a) In study 1, neural patterns of the dmPFC and a small part of the vmPFC represented subjective value independent of the task. (b) In study 2, only the dmPFC was found to represent task-independent value information. (c) The results of the two studies converged in a cluster in the dmPFC.

value represented in the dmPFC might generalize across cost types and datasets. Although less is known about multivariate representation of subjective value in effort-based decision-making, our findings align closely with previous MVPA studies showing subjective value signals in the dmPFC across other decision-making tasks (e.g., intertemporal and risky) and different reward categories (Gross et al., 2014; Piva et al., 2019; Pogoda et al., 2016). Most previous studies focused on the role of the vmPFC in domain-general value integration (Bartra et al., 2013; Clithero and Rangel, 2014; Levy and Glimcher, 2012; Peters and Büchel, 2009). Our cross-task MVPA findings suggest that the dmPFC may also be critically involved in calculating subjective value regardless of task type.

As mentioned above, the vmPFC has been regarded as a potential hub for task-independent subjective value representation (Levy and Glimcher, 2012) since a plethora of research has demonstrated neural correlates of value in this region across different reward types and valuation stages (Bartra et al., 2013; Clithero and Rangel, 2014; Kahnt et al., 2014; Sescousse et al., 2013; Smith et al., 2010). Indeed, both univariate and multivariate analyses showed neural correlates of subjective value in the vmPFC in study 1. However, some analyses did not

identify significant value signals in the vmPFC and anterior dmPFC in study 2. These inconsistent results may be related to the differences in the task design since participants can focus on computing the value of the single option in study 1 but may have relied on additional cognitive processes (e.g., attention distribution) in study 2 because two options were represented simultaneously in each trial (Arulpragasam et al., 2018; Westbrook et al., 2019). Moreover, the blood oxygenation level-dependent signal around the vmPFC is likely to be affected by susceptibility gradients, and these influences could be reduced by changing the scanning orientation (Deichmann et al., 2003), as implemented in study 1. A potential limitation of study 2 is that it did not use this optimized orientation when collecting functional images. Hence, future studies on valuation processes related to vmPFC activity should thus consider changing the imaging slice orientation to reduce related signal dropout.

A broader question that follows from these considerations is whether the dmPFC and vmPFC play a similar role in value integration. A popular hypothesis proposes that the vmPFC is mainly involved in computing the net value of potential outcomes associated with an option (also referred to as stimulus value in some cases). Accordingly, this signal gets passed on to the dmPFC to compute action value (similar to subjective value used in the current study) by subtracting related costs from it (Rangel and Hare, 2010; Rushworth and Behrens, 2008; Shenhav et al., 2016). Indeed, we found that the dmPFC can independently represent both outcomes and effort levels, supporting its role in integrating these two components during effort-based decision-making. Alternatively, other researchers argued that the dmPFC is more likely to encode prediction error to guide value integration in the vmPFC during decision-making (Arulpragasam et al., 2018; Vassena et al., 2020, 2014). Most of these studies were based on a sequential decision-making task and univariate fMRI analyses. Future studies using other neural measurements and multivariate analyses are needed to elucidate the role of the dmPFC when prediction error and subjective value are dissociable. Finally, another possibility is that value integration during decision-making is achieved by a joint effort of a small number of regions (Hunt and Hayden, 2017). This mechanism reduces the risk of completely losing the ability to integrate values when a core site (e.g., vmPFC) inside the network is disrupted (Yu et al., 2022). Taken together, the precise role of the dmPFC in value integration and how it interacts with the vmPFC during decision-making remain to be open questions that deserve further investigation (Fatahi et al., 2020).

5. Conclusions

In summary, our study indicates that effort discounting can be best described by a two-parameter power function. Using multivariate fMRI analysis, we found that the activity patterns of the dmPFC can represent subjective value across effort-based and risky decision-making, and the results are robust across two independent studies. Overall, the work we present here advances our understanding of the neural and computational mechanisms underlying effort-related value integration and suggests that the dmPFC emerges as a potential hub that utilizes a task-independent mechanism for computing subjective value.

Data and code availability statement

Behavioral data and analysis code are available on the Open Science Framework (https://osf.io/qdmyx/). Imaging data for study 1 are available on https://openneuro.org/datasets/ds003782/. Imaging data for study 2 are not openly available due to ethical restrictions, but are available upon request to the corresponding authors with a data sharing agreement in accordance with the conditions of the local ethics committee.

CRediT authorship contribution statement

Yuan-Wei Yao: Conceptualization, Methodology, Formal analysis, Data curation, Writing – original draft, Visualization, Project administration. **Kun-Ru Song:** Software, Formal analysis, Investigation, Writing – review & editing. **Nicolas W. Schuck:** Methodology, Visualization, Writing – review & editing. **Xin Li:** Investigation, Writing – review & editing. **Xiao-Yi Fang:** Conceptualization, Resources, Writing – review & editing. **Jin-Tao Zhang:** Conceptualization, Resources, Writing – review & editing, Supervision, Funding acquisition. **Hauke R. Heekeren:** Conceptualization, Writing – review & editing, Supervision. **Rasmus Bruckner:** Methodology, Formal analysis, Data curation, Writing – review & editing, Visualization, Supervision.

Declaration of Competing Interest

The authors declare no conflict of interest.

Acknowledgments

This research was supported by the National Natural Science Foundation of China (No. 32171083 and No. 31871122). Y.W.Y. was supported by the Einstein Center for Neurosciences Berlin. N.W.S. was funded by a Starting Grant from the European Union (ERC-StG-REPLAY-852669), and an Independent Max Planck Research Group grant awarded by the Max Planck Society (M.TN.A.BILD0004) and the Excellence Strategy of the Federal Government and the Länder. The funders had no role in study design, data collection and analysis, decision to publish, or preparation of the manuscript. We would like to thank Andrew Westbrook, Romy Frömer, and Jan Gläscher for helpful suggestions and Nadav Aridan and Tom Schonberg for sharing the choice and fMRI data of study 1.

Supplementary materials

Supplementary material associated with this article can be found, in the online version, at doi:10.1016/j.neuroimage.2023.120326.

References

Ahn, W.Y., Haines, N., Zhang, L., 2017. Revealing neurocomputational mechanisms of reinforcement learning and decision-making with the hBayesDM package. Comput. Psychiatry 1. https://doi.org/10.1162/cpsy_a_00002.

Aridan, N., Malecek, N.J., Poldrack, R.A., Schonberg, T., 2019. Neural correlates of effort-based valuation with prospective choices. Neuroimage 185, 446–454.

Arulpragasam, A.R., Cooper, J.A., Nuutinen, M.R., Treadway, M.T., 2018. Corticoinsular circuits encode subjective value expectation and violation for effortful goal-directed behavior. Proc. Natl. Acad. Sci. 115, E5233–E5242.

Bartra, O., McGuire, J.T., Kable, J.W., 2013. The valuation system: a coordinate-based meta-analysis of BOLD fMRI experiments examining neural correlates of subjective value. Neuroimage 76, 412–427.

Brassard, S.L., Balodis, I.M., 2021. A review of effort-based decision-making in eating and weight disorders. Prog. Neuropsychopharmacol. Biol. Psychiatry 110, 110333.

Chong, T.T.J., Apps, M., Giehl, K., Sillence, A., Grima, L.L., Husain, M., 2017. Neurocomputational mechanisms underlying subjective valuation of effort costs. PLoS Biol. 15, e1002598.

Clithero, J.A., Rangel, A., 2014. Informatic parcellation of the network involved in the computation of subjective value. Soc. Cogn. Affect. Neurosci. 9, 1289–1302.

Deichmann, R., Gottfried, J.A., Hutton, C., Turner, R., 2003. Optimized EPI for fMRI studies of the orbitofrontal cortex. Neuroimage 19, 430–441. https://doi.org/10.1016/S1053-8119(03)00073-9.

Escobar, G.G., Morales-Chainé, S., Haynes, J.M., Santoyo, C., Mitchell, S.H., 2023. Moderate stability among delay, probability, and effort discounting in humans. Psychol. Rec. 73, 1–14.

Fatahi, Z., Ghorbani, A., Zibaii, M.I., Haghparast, A., 2020. Neural synchronization between the anterior cingulate and orbitofrontal cortices during effort-based decision making. Neurobiol. Learn. Mem. 175, 107320.

Frömer, R., Shenhav, A., 2021. Filling the gaps: cognitive control as a critical lens for understanding mechanisms of value-based decision-making. Neurosci. Biobehav. Rev.

Gold, J.M., Waltz, J.A., Frank, M.J., 2015. Effort cost computation in schizophrenia: a commentary on the recent literature. Biol. Psychiatry 78, 747–753.

Gross, J., Woelbert, E., Zimmermann, J., Okamoto-Barth, S., Riedl, A., Goebel, R., 2014. Value signals in the prefrontal cortex predict individual preferences across reward categories. J. Neurosci. 34, 7580–7586.
Harris, S., Bray, S.R., 2021. Mental fatigue, anticipated effort, and subjective valuations of exercising predict choice to exercise or not: a mixed-methods study. Psychol. Sport Exerc. 54, 101924.
Haynes, J.D., Rees, G., 2006. Decoding mental states from brain activity in humans. Nat. Rev. Neurosci. 7, 523–534.
Hebart, M.N., Görgen, K., Haynes, J.D., 2015. The Decoding Toolbox (TDT): a versatile software package for multivariate analyses of functional imaging data. Front. Neuroinform. 8, 88.
Hogan, P.S., Galaro, J.K., Chib, V.S., 2019. Roles of ventromedial prefrontal cortex and anterior cingulate in subjective valuation of prospective effort. Cereb. Cortex 29, 4277–4290.
Hunt, L.T., Hayden, B.Y., 2017. A distributed, hierarchical and recurrent framework for reward-based choice. Nat. Rev. Neurosci. 18, 172–182.
Huys, Q.J.M., Cools, R., Gölzer, M., Friedel, E., Heinz, A., Dolan, R.J., Dayan, P., 2011. Disentangling the roles of approach, activation and valence in instrumental and pavlovian responding. PLoS Comput. Biol. 7, e1002028.
Jimura, K., Poldrack, R.A., 2012. Analyses of regional-average activation and multivoxel pattern information tell complementary stories. Neuropsychologia 50. https://doi.org/10.1016/j.neuropsychologia.2011.11.007.
Kable, J.W., Glimcher, P.W., 2007. The neural correlates of subjective value during intertemporal choice. Nat. Neurosci. 10, 1625–1633.
Kahneman, D., Tversky, A., 1979. Prospect theory: an analysis of decision under risk. Econometrica 47, 263–292.
Kahnt, T., Park, S.Q., Haynes, J.D., Tobler, P.N., 2014. Disentangling neural representations of value and salience in the human brain. Proc. Natl. Acad. Sci. U. S. A. 111 https://doi.org/10.1073/pnas.1320189111.
Kahnt, T., 2018. A decade of decoding reward-related fMRI signals and where we go from here. Neuroimage 180. https://doi.org/10.1016/j.neuroimage.2017.03.067.
Klein-Flügge, M.C., Kennerley, S.W., Saraiva Ana, C., Penny, W.D., Bestmann, S., 2015. Behavioral modeling of human choices reveals dissociable effects of physical effort and temporal delay on reward devaluation. PLoS Comput. Biol. 11 https://doi.org/10.1371/journal.pcbi.1004116.
Klein-Flügge, M.C., Kennerley, S.W., Friston, K., Bestmann, S., 2016. Neural signatures of value comparison in human cingulate cortex during decisions requiring an effort-reward trade-off. J. Neurosci. 36, 10002–10015.
Kolling, N., Wittmann, M.K., Behrens, T.E.J., Boorman, E.D., Mars, R.B., Rushworth, M.F. S., 2016. Value, search, persistence and model updating in anterior cingulate cortex. Nat. Neurosci. 19, 1280–1285.
Levy, D.J., Glimcher, P.W., 2012. The root of all value: a neural common currency for choice. Curr. Opin. Neurobiol. 22, 1027–1038.
Lockwood, P.L., Klein-Flügge, M.C., 2021. Computational modelling of social cognition and behaviour—a reinforcement learning primer. Soc. Cogn. Affect. Neurosci. 16, 761–771.
Lockwood, P.L., Hamonet, M., Zhang, S.H., Ratnavel, A., Salmony, F.U., Husain, M., Apps, M.A.J., 2017. Prosocial apathy for helping others when effort is required. Nat. Hum. Behav. 1, 1–10.
Lockwood, P.L., Wittmann, M.K., Nili, H., Matsumoto-Ryan, M., Abdurahman, A., Cutler, J., Husain, M., Apps, M.A.J., 2022. Distinct neural representations for prosocial and self-benefiting effort. Curr. Biol. 32, 4172–4185.
Lopez-Gamundi, P., Yao, Y.W., Chong, T.T.J., Heekeren, H.R., Mas-Herrero, E., Marco-Pallarés, J., 2021. The neural basis of effort valuation: a meta-analysis of functional magnetic resonance imaging studies. Neurosci. Biobehav. Rev. 131, 1275–1287.
Massar, S.A.A., Libedinsky, C., Weiyan, C., Huettel, S.A., Chee, M.W.L., 2015. Separate and overlapping brain areas encode subjective value during delay and effort discounting. Neuroimage 120, 104–113.
Meyniel, F., Goodwin, G.M., Deakin, J.F.W., Klinge, C., MacFadyen, C., Milligan, H., Mullings, E., Pessiglione, M., Gaillard, R., 2016. A specific role for serotonin in overcoming effort cost. eLife 5, e17282.
Nee, D.E., Kastner, S., Brown, J.W., 2011. Functional heterogeneity of conflict, error, task-switching, and unexpectedness effects within medial prefrontal cortex. Neuroimage 54, 528. https://doi.org/10.1016/j.neuroimage.2010.08.027. -40.
Neubert, F.X., Mars, R.B., Sallet, J., Rushworth, M.F.S., 2015. Connectivity reveals relationship of brain areas for reward-guided learning and decision making in human and monkey frontal cortex. Proc. Natl. Acad. Sci. 112, E2695–E2704.
Nilsson, H., Rieskamp, J., Wagenmakers, E.J., 2011. Hierarchical Bayesian parameter estimation for cumulative prospect theory. J. Math. Psychol. 55, 84–93.
Pachur, T., Mata, R., Hertwig, R., 2017. Who dares, who errs? Disentangling cognitive and motivational roots of age differences in decisions under risk. Psychol. Sci. 28, 504–518.
Peters, J., Büchel, C., 2009. Overlapping and distinct neural systems code for subjective value during intertemporal and risky decision making. J. Neurosci. 29, 15727–15734.
Piva, M., Velnoskey, K., Jia, R., Nair, A., Levy, I., Chang, S.W.C., 2019. The dorsomedial prefrontal cortex computes task-invariant relative subjective value for self and other. eLife 8, e44939.
Pogoda, L., Holzer, M., Mormann, F., Weber, B., 2016. Multivariate representation of food preferences in the human brain. Brain Cogn. 110, 43–52.
Prévost, C., Pessiglione, M., Météreau, E., Cléry-Melin, M.L., Dreher, J.C., 2010. Separate valuation subsystems for delay and effort decision costs. J. Neurosci. 30, 14080–14090. https://doi.org/10.1523/JNEUROSCI.2752-10.2010.
Rangel, A., Hare, T., 2010. Neural computations associated with goal-directed choice. Curr. Opin. Neurobiol. 20, 262–270. https://doi.org/10.1016/j.conb.2010.03.001.
Rudebeck, P.H., Behrens, T.E., Kennerley, S.W., Baxter, M.G., Buckley, M.J., Walton, M. E., Rushworth, M.F.S., 2008. Frontal cortex subregions play distinct roles in choices between actions and stimuli. J. Neurosci. 28, 13775–13785.
Rushworth, M.F.S., Behrens, T.E.J., 2008. Choice, uncertainty and value in prefrontal and cingulate cortex. Nat. Neurosci. 11, 389–397.
Sayalı, C., Badre, D., 2019. Neural systems of cognitive demand avoidance. Neuropsychologia 123, 41–54.
Seaman, K.L., Brooks, N., Karrer, T.M., Castrellon, J.J., Perkins, S.F., Dang, L.C., Hsu, M., Zald, D.H., Samanez-Larkin, G.R., 2018. Subjective value representations during effort, probability and time discounting across adulthood. Soc. Cogn. Affect. Neurosci. 13, 449–459. https://doi.org/10.1093/scan/nsy021.
Sescousse, G., Caldú, X., Segura, B., Dreher, J.C., 2013. Processing of primary and secondary rewards: a quantitative meta-analysis and review of human functional neuroimaging studies. Neurosci. Biobehav. Rev. 37, 681–696.
Shenhav, A., Cohen, J.D., Botvinick, M.M., 2016. Dorsal anterior cingulate cortex and the value of control. Nat. Neurosci. 19, 1286–1291.
Smith, D.V., Hayden, B.Y., Truong, T.K., Song, A.W., Platt, M.L., Huettel, S.A., 2010. Distinct value signals in anterior and posterior ventromedial prefrontal cortex. J. Neurosci. 30, 2490–2495.
Soutschek, A., Nadporozhskaia, L., Christian, P., 2022. Brain stimulation over dorsomedial prefrontal cortex modulates effort-based decision making. Cogn. Affect. Behav. Neurosci. 22, 1264–1274.
Todd, M.T., Nystrom, L.E., Cohen, J.D., 2013. Confounds in multivariate pattern analysis: theory and rule representation case study. Neuroimage 77, 157–165.
Treadway, M.T., Bossaller, N.A., Shelton, R.C., Zald, D.H., 2012. Effort-based decision-making in major depressive disorder: a translational model of motivational anhedonia. J. Abnorm. Psychol. 121, 553.
Tversky, A., Kahneman, D., 1992. Advances in prospect theory: cumulative representation of uncertainty. J. Risk Uncertain. 5, 297–323.
Vassena, E., Krebs, R.M., Silvetti, M., Fias, W., Verguts, T., 2014. Dissociating contributions of ACC and vmPFC in reward prediction, outcome, and choice. Neuropsychologia 59, 112–123.
Vassena, E., Deraeve, J., Alexander, W.H., 2020. Surprise, value and control in anterior cingulate cortex during speeded decision-making. Nat. Hum. Behav. 4, 412–422.
Vehtari, A., Gelman, A., Gabry, J., 2017. Practical Bayesian model evaluation using leave-one-out cross-validation and WAIC. Stat. Comput. 27, 1413–1432.
Venkatraman, V., Payne, J.W., Bettman, J.R., Luce, M.F., Huettel, S.A., 2009. Separate neural mechanisms underlie choices and strategic preferences in risky decision making. Neuron 62, 593–602.
Von Neumann, J., Morgenstern, O., 1944. Theory of games and economic behavior. Theory of Games and Economic Behavior. Princeton university press.
Walton, M.E., Groves, J., Jennings, K.A., Croxson, P.L., Sharp, T., Rushworth, M.F.S., Bannerman, D.M., 2009. Comparing the role of the anterior cingulate cortex and 6-hydroxydopamine nucleus accumbens lesions on operant effort-based decision making. Eur. J. Neurosci. 29, 1678–1691.
Wang, Q., Luo, S., Monterosso, J., Zhang, J., Fang, X., Dong, Q., Xue, G., 2014. Distributed value representation in the medial prefrontal cortex during intertemporal choices. J. Neurosci. 34, 7522–7530.
Westbrook, A., Kester, D., Braver, T.S., 2013. What is the subjective cost of cognitive effort? Load, trait, and aging effects revealed by economic preference. PLoS One 8. https://doi.org/10.1371/journal.pone.0068210.
Westbrook, A., Lamichhane, B., Braver, T., 2019. The subjective value of cognitive effort is encoded by a domain-general valuation network. J. Neurosci. 39, 3934–3947.
Westbrook, A., van den Bosch, R., Määttä, J.I., Hofmans, L., Papadopetraki, D., Cools, R., Frank, M.J., 2020. Dopamine promotes cognitive effort by biasing the benefits versus costs of cognitive work. Science 1979 (367), 1362–1366.
Wilson, R.C., Collins, A.G.E., 2019. Ten simple rules for the computational modeling of behavioral data. eLife 8, e49547.
Yan, C.G., Wang, X.D., Zuo, X.N., Zang, Y.F., 2016. DPABI: data processing & analysis for (resting-state) brain imaging. Neuroinformatics 14, 339–351.
Yao, Y., Vehtari, A., Simpson, D., Gelman, A., 2018. Using stacking to average Bayesian predictive distributions (with discussion). Bayesian Anal. 13, 917–1007.
Yu, L.Q., Dana, J., Kable, J.W., 2022. Individuals with ventromedial frontal damage display unstable but transitive preferences during decision making. Nat. Commun. 13, 4758.
Zhang, L., Lengersdorff, L., Mikus, N., Gläscher, J., Lamm, C., 2020. Using reinforcement learning models in social neuroscience: frameworks, pitfalls and suggestions of best practices. Soc. Cogn. Affect. Neurosci. 15, 695–707.